DISTRIBUTED FEEDBACK LASERS

Distributed feedback (DFB) lasers are a special class of semiconductor diode lasers. They have found widespread application in fiber optic telecommunication systems, where they are essential for the operation of long-haul fiber links. DFB lasers have a much narrower wavelength emission spectrum compared to the conventional diode lasers, and they emit light essentially at a single wavelength. For this reason they are also referred to as single frequency lasers. Diode lasers operate on the same "amplification of stimulated emission" principle as other laser systems. To achieve this light amplification, lasers are composed of a gain medium inserted between two mirrors. The mirrors provide the positive feedback needed to initiate laser action, as external excitation is applied to the active medium. This configuration of an active region and mirrors is referred to as the laser cavity. The mirrors are generally not completely reflecting, so some amount of light leaks out and is collected as output from the cavity. As the active medium is excited, or pumped, the excitation is converted to light by the gain medium. The light begins to propagate within the cavity formed by the mirrors and the optical field starts to build up in intensity. Laser action begins once there is enough light to overcome the cavity and mirror losses.

In a typical laser cavity, the feedback from the mirrors is broadband and is not wavelength selective. A passive cavity, that is, in the absence of the gain region, is a resonator which, in principle, will support an infinite number of oscillating modes. In a laser, the wavelength of operation depends on the range of wavelengths over which the active medium can provide useful gain. Diode lasers of this type are referred to as Fabry–Perot (FP) lasers. They generally operate at several different wavelengths or longitudinal (the direction along the cavity) modes. This type of laser is acceptable for many applications except in those where the dispersion in the optical fiber becomes detrimental. The mode index (which is a combination of the material refractive index and contributions from the waveguiding structure) of the optical fiber varies as a function of the wavelength of light propagating in it. This variation in index, which is commonly referred to as fiber dispersion, causes different wavelengths to propagate down the optical fiber at different speeds. When the laser signal, which is composed of several different wavelengths from a FP laser transmitter, reaches the receiver, after traveling some distance in the optical fiber, it is spread out in time. This results in signal distortion, called the intersymbol interference, and severely limits the transmission distance of fiber optic systems. To limit dispersion-induced distortion, one needs a laser source with a narrow emission spectrum.

Emission spectrum of FP lasers can be considerably narrowed by providing wavelength-selective feedback. In DFB lasers, such a wavelength-selective feedback is provided within and throughout the laser cavity. This type of feedback can also be provided by wavelength-selective mirrors. Such a laser is called the distributed bragg reflector (DBR) laser. The DBR laser is a diverse subject in itself and will not be discussed here. FP lasers that are externally stabilized using a grating to provide wavelength-selective feedback also fall into this category. The external grating may also be written on the fiber used to couple light out of a diode laser in a package. Frequency-tunable lasers can be made using external gratings. The wavelength of the feedback into the laser cavity is adjusted by changing the orientation of the grating with respect to the laser cavity and, by continually changing the orientation of the grating, the laser output can be tuned over a wide range of frequencies.

DFB DEVICE STRUCTURE AND MATERIAL CHARACTERISTICS

Electrically, semiconductor lasers are equivalent to p–n junction diodes. They are composed of a vertically (or laterally) stacked p and n heterojunction sandwich. The excitation is provided by injecting electrical current in a forward-biased configuration. The current flow is bipolar, that is, the current transport is composed of both electrons and holes. The heterojunction is necessary to confine the bipolar carriers in the same spatial location for efficient recombination, thereby reducing the threshold necessary to overcome cavity losses for laser action. An electron recombines with a hole to produce a photon. The first-generation diode lasers were of the homojunction type and required very large pump excitation for laser action.

Figure 1 shows a drawing of a modern buried heterostructure DFB semiconductor laser diode. "Buried" refers to the fact that the p–n heterojunction gain region of the laser has been completely surrounded by another material. This minimizes the material index variation adjacent to the active region, and it has some desirable waveguide properties for the optical mode within the cavity. The wavelength-selective feedback in the cavity is provided by the mode index or gain/loss variations caused by the grating etched into the semiconductor material. $InP/In_{1-x}Ga_xAs_yP_{1-y}$ material alloy combination is typically used to make DFB lasers for telecommunication applications. Lasers made of this material combination emit light in the 1.2 μm to 1.6 μm wavelength. Although DFB lasers have been made from other material systems, most are from $GaAs/Al_xGa_{1-x}$. As alloys emitting light in the 0.75 μm to 0.85 μm region, these have not found use in long-distance data transmission due to the loss and dispersion characteristics of the commonly used silica optical fiber. This discussion will only be concerned with the InP based or, more commonly called, the long-wavelength DFB lasers.

Figure 1 also shows the conduction band energy diagram of three possible types of active regions. In all three cases the light-emitting layer, the one in the middle (usually made of the InGaAs alloy) has the lowest bandgap energy. The outermost cladding regions are usually composed of InP and these layers have the largest bandgap energies. This combination of materials with different bandgap energies to form the p–n junction is referred to as a heterojunction. In a homojunction

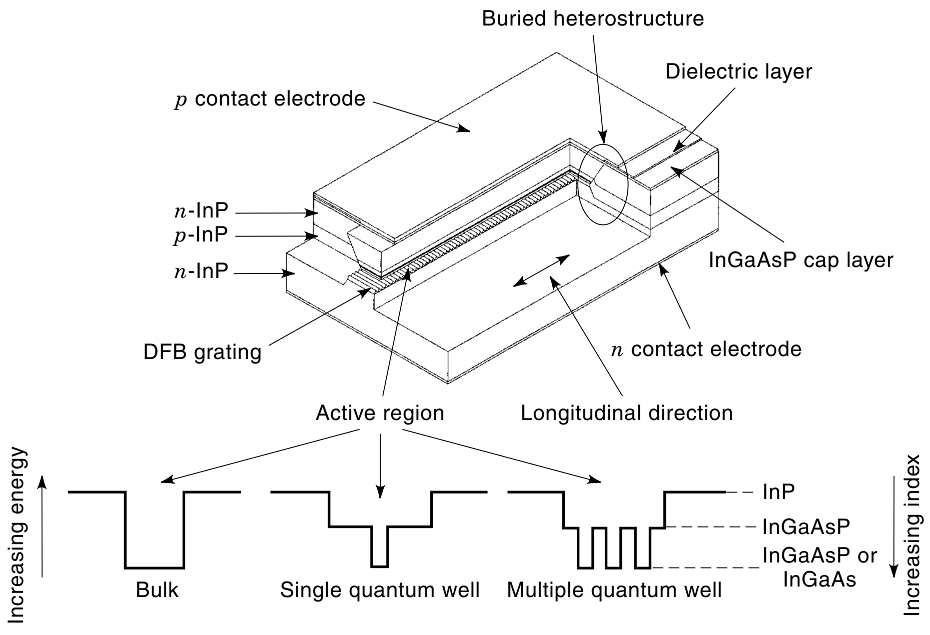

Figure 1. Cut-away drawing of a buried heterostructure DFB laser. The active region is the layer above the grating. The doping sequence for the laser structure is *p-active region-n* from the top to bottom. The sequence for the "burying" structure is the reverse. In addition to providing good waveguiding properties, the reverse doping sequence of the "burying" structure forms a current blocking region, thereby channeling the injected current, under forward bias, directly into the active region. The details of the active region conduction band energy structure are also shown. The material layer between two quantum wells is called the barrier. The width of the layer between the outer cladding and the first quantum well is usually varied to provide maximum overlap between the quantum wells and the optical mode in the cavity. This type of design is called the separate confinement heterostructure. The total width of the confinement heterostructure (all the layers between the outer InP cladding layers) is about 0.2 μm (of the order of the width of the bulk active region).

laser, the cladding and active regions have the same bandgap energies and no electric potential is present to confine the carriers and facilitate their recombination. In Fig. 1, it is easy to visualize the carriers "tumbling" down the energy potential of the active region to the lowest level before recombining to emit light. In the bulk active region, the layer width is typically between 0.1 μm and 0.2 μm. In this case, the carriers are unconfined in all three dimensions. As the width of the active layer (the smallest bandgap layer in Fig. 1) shrinks to about 0.01 μm, the carriers are quantum mechanically confined in the direction of the smallest dimension, but are free to move in the plane vertical to the paper. These are called quantum well lasers. Quantum well lasers can either have single or multiple wells. InP lasers, in general, tend to have multiple quantum wells (between 4 and 7). Although the cladding regions are p and n doped, the active region proper is nominally undoped. The active region is grown such that it is lattice matched to all the other layers. Doping and strain (by deliberate lattice mismatching of the active region) may be introduced into the active region. If done correctly, strained quantum well lasers and lasers with moderately doped active regions have a number of useful properties, like lower threshold current, narrower linewidth, and higher direct modulation bandwidth.

Figure 2 shows the attenuation characteristics of the silica fiber most commonly used in fiber optic transmission. The minimum in the loss characteristics occur at about the 1.55 μm wavelength, and hence, the relevance of DFB lasers emitting at this wavelength. The window at 1.3 μm wavelength is traditionally significant because the dispersion of the standard step index optical fiber goes to "zero" at this wavelength (technically, it is the first-order dispersion term that goes to zero at this wavelength, but dispersion has other higher-order terms that then become significant). In modern fibers this wavelength, also call the zero dispersion wavelength, can be tailored to match the loss minimum at 1.55 μm. This type of optical fiber is called the dispersion shifted fiber.

The very strong interest in the 1.5 μm region is also due to the ready availability of erbium-doped fiber amplifiers (EDFA) for boosting signals at this wavelength. Similarly, praseodymium-doped fiber amplifiers (PDFA) can be used to boost signals in the 1.3 μm wavelength region. The amplification bands for both wavelength regions have been superimposed on the fiber attenuation characteristics in Fig. 2.

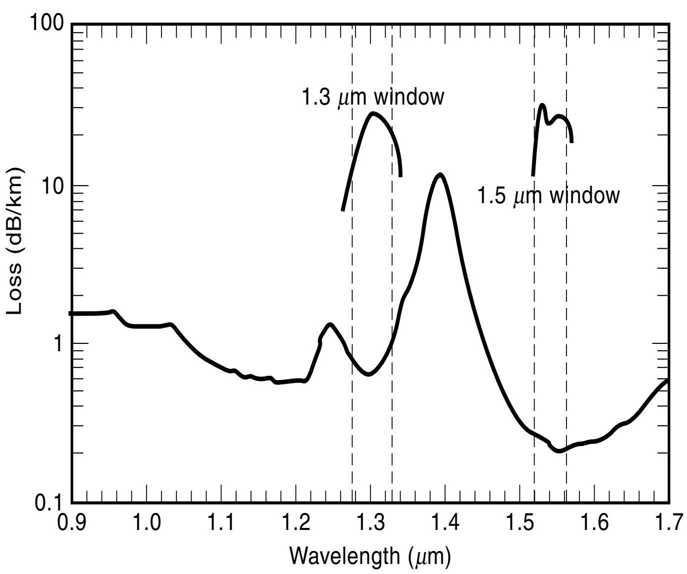

Figure 2. Attenuation characteristics of the silica fiber which is commonly deployed in the ground. The loss minimum occurs at around 1.55 μm wavelength. The peaks in the absorption curve near the 1.3 μm region is due to the hydroxyl ions (water), which are incorporated as impurities in the fiber during fabrication. The optical transmission windows at 1.3 μm and 1.5 μm wavelengths are also shown. These lines are merely to show the bandwidth of the windows and are not indicative of any loss values.

WAVELENGTH DIVISION MULTIPLEXING

The fiber has a very large bandwidth for signal transmission. The advent of fiber-based optical amplifiers and other fiber-based devices has made it possible to realize this bandwidth over very large transmission distances. One way of utilizing this huge bandwidth is to use wavelength division multiplexing (WDM). Since it is impossible, at least for the present generation of electronics, to take full advantage of all the usable fiber bandwidth, WDM systems employ lasers at several different wavelengths, each carrying a high-speed data signal. This is analogous to the subcarrier division multiplexed systems in the microwave domain. For instance, the conventional amplification band in the EDFA is about 32 nm wide. Current commercial transmission systems can accommodate signals spaced at 100 GHz or 0.8 nm apart for a total of 40 channels. Each of these channels run at the SONET (Synchronous Optical Network) OC-48 standard data rate of 2.48832 Gbit/s for an aggregate data rate close to 100 Gbit/s. There are proposals to halve the channel spacing and quadruple the data rate for an eightfold increase in data throughput to 800 Gbit/s in a single silica fiber. This data throughput can be further enhanced with the new generation EDFAs, which, in laboratory tests, have demonstrated as much as 80 nm bandwidth in the 1.5 μm wavelength region. As the wavelengths are packed together for higher and higher data throughput, the term dense WDM (DWDM) systems is coming into common usage. Modern-day DWDM systems increasingly need DFB lasers with tighter wavelength control and higher spectral purity (this translates to a requirement for narrow linewidth or low phase noise DFB lasers) for proper implementation. The ultimate limit to DWDM systems is the coherent transmission system.

A review of the current state-of-the-art in components for optical fiber telecommunication systems may be found in the two volume set edited by Kaminow and Koch (1). Two good textbooks in the area of semiconductor lasers are by Coldren and Corzine (2), and Agrawal and Dutta (3).

ANALYTIC TREATMENT

Distributed Feedback Model

Detailed analysis of a DFB laser is complicated, and is only possible using numerical techniques. We present an analytic model which explains all major properties of DFB lasers without having to use numerical techniques. We follow the analysis used in the seminal paper on this subject by Kogelnik and Shank (4). The idea is not to replicate their work, but to provide an overview of the analysis and also supply a number of missing steps in the derivation that may prove useful to the reader. Starting point of the analysis is the scalar wave equation for the electric field.

$$\frac{\partial E^2}{\partial z^2} + k^2 E = 0 \tag{1}$$

where E is the complex amplitude of the electric field. This field varies with angular frequency ω. The propagation constant, k, can be written as

$$k^2 = \omega^2 \mu\epsilon = \omega^2 \mu_0 \epsilon_0 (\epsilon_r + j\epsilon_i) = k_0^2 (\epsilon_r + j\epsilon_i) \tag{2}$$

where $k_0^2 = \omega^2 \mu_0 \epsilon_0$ is the propagation constant in the vacuum and the complex permittivity, ϵ_{tot}, of the medium has been written as a sum of its real and imaginary parts. Consider a nonmagnetic dielectric medium, $\mu = \mu_0$. If the refractive index of the medium is n and the gain in the medium is α (in units of inverse length), then the complex refractive index of the medium, n_{tot}, can be written as

$$n_{\text{tot}} = n + j\frac{\alpha\lambda}{2\pi} \tag{3}$$

Assuming that the gain is small over distance of the order of a wavelength, $\alpha\lambda/2\pi \ll n$,

$$\epsilon_{\text{tot}} = n_{\text{tot}}^2 \approx n^2 + j\frac{\alpha n \lambda}{\pi} \tag{4}$$

The expression for k^2 in Eq. (2) can then be written as

$$k^2 = k_0^2 n^2 \left(1 + j\frac{\alpha\lambda}{n\pi}\right) = k_0^2 n(z)^2 \left(1 + j\frac{2\alpha(z)}{k_0 n(z)}\right) \tag{5}$$

where $k_0 = 2\pi/\lambda$. In a DFB structure, both n and α vary periodically, and they are taken to be a function of the z coordinate, that is, the longitudinal direction in the laser. The periodic spatial variation of the index and gain along the z direction in a DFB laser cavity can be written as

$$\begin{aligned} n(z) &= n_o + \Delta n \cos(2\beta_0 z) \\ \alpha(z) &= \alpha_o + \Delta\alpha \cos(2\beta_0 z) \end{aligned} \tag{6}$$

where β_0 is the propagation constant of the waves at the Bragg condition. If Λ_0 is the period of the distributed feedback structure, $\beta_0 = \pi/\Lambda_0$. At the Bragg condition,

$$\beta_0 \equiv \frac{\pi}{\Lambda_0} = \frac{2\pi}{\lambda/n_0} \tag{7}$$

which implies that the spatial periodicity, Λ_0, is equal to half the wavelength of the light in the medium, $(\lambda/2)/n_0$. This is an important result for all devices that depend on some form of a distributed reflector for their operation. Although this result has been assumed here, it can shown to be true using Fourier analysis of wave propagation in periodic structures (2). Substituting Eq. (6) into Eq. (5), one obtains the following expression for the propagation constant:

$$k^2 \approx \beta^2 + 2j\beta\alpha_0 + 4\beta\left[\frac{\pi\Delta n}{\lambda} + j\frac{\Delta\alpha}{2}\right]\cos(2\beta_0 z) \tag{8}$$

In deriving the expression for k in Eq. (8), $\beta = k_0 n_0$ and is assumed that $\Delta n \ll n_0$, $\Delta\alpha \ll \alpha_0$, and $\alpha_0 \ll \beta_0$. Equation (8) can be rewritten in terms of a coupling constant κ as

$$\begin{aligned} k^2 &\approx \beta^2 + 2j\beta\alpha_0 + 4\kappa\beta\cos(2\beta_0 z) \\ &= \beta^2 + 2j\beta\alpha_0 + 2\kappa\beta(e^{-2j\beta_0} + e^{2j\beta_0}) \\ \kappa &\equiv \kappa_r + j\kappa_i = \frac{\pi\Delta n}{\lambda} + j\frac{\Delta\alpha}{2} \end{aligned} \tag{9}$$

The coupling constant κ defines the strength of the feedback provided by the gratings in the DFB laser. The expression for k^2 can then be substituted into the scalar wave, Eq. (1).

Coupled Wave Description

The scalar wave equation, in principle, will have an infinite set of solutions each corresponding to a certain diffraction order of the propagating wave. Consider the lowest-order solution to the equation close to the Bragg frequency. This corresponds to a forward -and-backward traveling wave. In the absence of any perturbation, these basic modes of the waveguide are orthogonal and do not couple, but in the presence of index and/or gain variations in the laser cavity they scatter into one another and form the basis of the coupled wave description of the DFB laser. The sum of the complex amplitudes of the forward-and-backward traveling waves, which will form the trial solution to the wave equation, is written as

$$E(z) = R(z)e^{-j\beta_0 z} + S(z)e^{j\beta_0 z} \tag{10}$$

Substituting Eq. (9) and Eq. (10) into Eq. (1),

$$\begin{aligned}&\left(\frac{\partial^2 R}{\partial z^2} - 2j\beta_0\frac{\partial R}{\partial z} - \beta_0^2 R + \beta^2 R + 2j\beta\alpha_0 R + 2\kappa\beta S\right)e^{-j\beta_0 z}\\&\quad + \left(\frac{\partial^2 S}{\partial z^2} + 2j\beta_0\frac{\partial S}{\partial z} - \beta_0^2 S + \beta^2 S + 2j\beta\alpha_0 S + 2\kappa\beta R\right)e^{j\beta_0 z}\\&\qquad + 2\kappa\beta R e^{-3j\beta_0 z} + 2\kappa\beta S e^{3j\beta_0 z} = 0\end{aligned} \tag{11}$$

Since it has been assumed that the perturbations in the gain and index of the medium are small, $\partial^2 R/\partial z^2$ and $\partial^2 S/\partial z^2$ can be neglected. If the coefficients of each of the harmonic components are independently set to zero, one obtains a pair of coupled-wave equations:

$$\begin{aligned}-\frac{\partial R}{\partial z} + \frac{\beta\alpha_0}{\beta_0}R - j\left(\frac{\beta^2-\beta_0^2}{2\beta_0}\right)R &= j\frac{\kappa\beta}{\beta_0}S\\ \frac{\partial S}{\partial z} + \frac{\beta\alpha_0}{\beta_0}S - j\left(\frac{\beta^2-\beta_0^2}{2\beta_0}\right)S &= j\frac{\kappa\beta}{\beta_0}R\end{aligned} \tag{12}$$

When the deviation from the Bragg frequency is small, the coupled wave equation can be simplified by setting $\beta/\beta_0 \approx 1$. A normalized frequency deviation parameter, δ, is then defined as

$$\delta = \left(\frac{\beta^2-\beta_0^2}{2\beta_0}\right) \approx \beta - \beta_0 = \frac{n_o(\omega-\omega_0)}{c} \tag{13}$$

With these simplifications, the coupled wave equations reduce to

$$\begin{aligned}-\frac{\partial R}{\partial z} + (\alpha_0 - j\delta)R &= j\kappa S\\ \frac{\partial S}{\partial z} + (\alpha_0 - j\delta)S &= j\kappa R\end{aligned} \tag{14}$$

where δ is the deviation of the oscillation frequency ω from the Bragg frequency ω_0. At the Bragg frequency, $\delta = 0$.

The coupled wave equations describe a forward-propagating wave that is first amplified by the medium. This wave is then scattered by the grating at frequencies close to the Bragg frequency into the backward-propagating wave. This scattered wave reinforces the backward-propagating wave in the cavity. Likewise, some of the backward-propagating wave is scattered into the forward-propagating wave. The boundary conditions at the facet play a large role in the steady-state evolution of the optical field within the laser cavity. To simplify the analysis here, assume that both facets are anti-reflection coated, that is, the forward-propagating wave is not reflected at the right-hand-side facet (thus not contributing to the initial value of the backward-propagating wave) and the backward-propagating wave is not reflected at the left-hand-side facet (thus not contributing to the initial value of the forward-propagating wave). These boundary conditions can be written as

$$R(-L/2) = S(L/2) = 0 \tag{15}$$

Here it has been assumed that the total cavity length is L extending from $z = -L/2$ to $z = L/2$. In a FP laser, the cleaved, uncoated, semiconductor crystal facets provide about 30% power feedback, which initiates and sustains laser action by overcoming the losses with the cavity. For all practical purposes, this feedback is uniform over all frequencies and such a laser is not wavelength selective. In the DFB structure, only frequencies at or close to the Bragg frequency will be supported by the cavity. If there is additional feedback from the facets (cleaved and uncoated) of the DFB laser, then the natural FP modes of the laser cavity will not be completely suppressed, leading to poor single-mode oscillation characteristics.

The wave equations in Eq. (14) can be rewritten as

$$\begin{aligned}\frac{\partial^2 R}{\partial z^2} - [\kappa^2 + (\alpha_0 - j\delta)^2]R &= 0\\ \frac{\partial^2 S}{\partial z^2} - [\kappa^2 + (\alpha_0 - j\delta)^2]S &= 0\end{aligned} \tag{16}$$

The general solution of these equations is of the form:

$$\begin{aligned}R &= r_1 e^{\gamma z} + r_2 e^{-\gamma z}\\ S &= s_1 e^{\gamma z} + s_2 e^{-\gamma z}\end{aligned} \tag{17}$$

where the complex propagation constant is given by

$$\gamma^2 = \kappa^2 + (\alpha_0 - j\delta)^2 \tag{18}$$

If γ is real then R and S will be purely evanescent waves and if γ is imaginary then R and S will form a standing wave within the cavity. Since it has been assumed that the device is symmetric, the solutions will be such that $E(-z) = E(z)$ and $E(-z) = -E(z)$. Using this and the boundary conditions, the solutions may be written as

$$\begin{aligned}R(z) &= \sinh[\gamma(z+L/2)] = (e^{\gamma(z+L/2)} - e^{-\gamma(z+L/2)})/2\\ S(z) &= \pm\sinh[\gamma(z-L/2)] = \pm(e^{\gamma(z-L/2)} - e^{-\gamma(z-L/2)})/2\end{aligned} \tag{19}$$

These equations describe the longitudinal distribution of the optical modes within the laser cavity. The forward-traveling wave, $R(z)$, builds up from zero at the left-hand end of the cavity at $z = -L/2$ to its maximum at the right-hand end of the cavity at $z = L/2$, and likewise the backward-traveling wave, $S(z)$, from the opposite end of the cavity.

Now to determine the set of eigenvalues γ for the cavity structure: This can be done by substituting Eq. (19) [taking the negative solution for $S(z)$] into Eq. (14). The sum and difference of the resulting equations are taken and the common terms are eliminated. The results is as follows:

$$-\gamma[e^{\gamma L/2}+e^{-\gamma L/2}]+(\alpha_o-j\delta)[e^{\gamma L/2}-e^{-\gamma L/2}] = j\kappa[e^{\gamma L/2}-e^{-\gamma L/2}]$$
$$-\gamma[e^{\gamma L/2}-e^{-\gamma L/2}]+(\alpha_o-j\delta)[e^{\gamma L/2}+e^{-\gamma L/2}] = j\kappa[e^{\gamma L/2}+e^{-\gamma L/2}] \tag{20}$$

Equation (20) can be again simplified by taking their sum and difference, to obtain Eq. (21):

$$\begin{aligned}\gamma-(\alpha_0-j\delta)&=j\kappa e^{-\gamma L}\\ \gamma+(\alpha_0-j\delta)&=-j\kappa e^{\gamma L}\end{aligned} \tag{21}$$

These equations can then be combined into one to obtain the complex transcendental equation for γ, which can then be numerically solved for the modes of the DFB structure. Each of these modes has its own threshold and lasing frequency corresponding to a particular cavity length and coupling strength of the grating.

Approximate Solutions

Several important results can be obtained without having to resort to a numerical solution of Eqs. (21). Invoke what is known as the high gain approximation to obtain these results.

The expressions for γ given in Eq. (18) can by simplified by using the high gain approximation, that is, $\alpha_0 \gg \kappa(=\kappa_r + j\kappa_i = \pi\Delta n/\lambda + j\Delta\alpha/2)$.

$$\gamma \approx \alpha_0 - j\delta \tag{22}$$

Substituting Eq. (22) into the second expression in Eq. (21),

$$2(\alpha_0-j\delta) = \pm j\kappa e^{(\alpha_0-j\delta)L} \tag{23}$$

Although the right-hand side of Eq. (23) is strictly negative, if one were to repeat the analysis starting at Eq. (19), taking the positive solution for $S(z)$, the result would be the positive solution for the right-hand side of Eq. (23). Equation (23) can then be solved to obtain the approximate solutions of the modes of the DFB structure.

First derive the phase condition that must be satisfied by the lasing modes in the cavity. This can be done by comparing the phase of both sides of Eq. (23).

$$\pm\tan^{-1}\left(\frac{\alpha_0}{\delta}\right) = \tan^{-1}\left(\frac{\kappa_i}{\kappa_r}\right) - \delta L \tag{24}$$

Near the Bragg frequency, one can assume $\delta \ll \alpha_0$. After substituting for δ from Eq. (13), Eq. (24) can be simplified to

$$\begin{aligned}\left(q+\frac{1}{2}\right)\pi &= \tan^{-1}\left(\frac{\kappa_i}{\kappa_r}\right) - \frac{2\pi n_0(v-v_o)}{c}L\\ \frac{v-v_o}{(c/2n_0L)} &= q+\frac{1}{2}+\frac{1}{\pi}\tan^{-1}\left(\frac{\kappa_i}{\kappa_r}\right)\end{aligned} \tag{25}$$

where $2\pi v = \omega$ and q is an integer such that $-\infty < q < \infty$.

The phase condition is central to the operation of the various classes of DFB lasers. The implications of the phase condition are listed below.

1. The cavity resonances are spaced approximately $c/2n_0L$ apart. This is like any other two mirror, Fabry–Perot laser cavity of length L.
2. Most conventional DFB lasers are purely index coupled, that is, $\Delta\alpha$, $\kappa_i = 0$. The lowest-order solution occurs for $q = -1, 0$ where $v_{-1} = v_o - c/4n_0L$, $v_o = v_o + c/4n_0L$. There is no solution at the Bragg frequency (v_o), and hence one has the problem of two degenerate modes in a conventional DFB structure, which are both equally likely to dominate unless something is done to break this degeneracy.
3. One way around the problem of two degenerate modes is to introduce a $\lambda/4$ additional phase shift within the cavity. For the index-coupled case, that modifies the phase condition as follows:

   $$\frac{v-v_o}{(c/2n_0L)} = q+1$$

   Now there is a resonance at the Bragg frequency, $v_{-1} = v_0$. This shift is introduced in the grating structure, and for symmetry reasons, it is usually done in the middle of the laser cavity during fabrication.
4. The second solution is to fabricate a gain (or loss) coupled DFB laser instead of the conventional index coupled one. In this case, Δn, $\kappa_r = 0$. This modifies the phase condition as follows:

   $$\frac{v-v_o}{(c/2n_0L)} = p+q+1$$

   where p and q are integers such that $-\infty < p, q < \infty$. Again there is a resonance at the Bragg frequency, $v_{0,-1} = v_{-1,0} = v_o$. Generally, most gain-coupled DFB lasers also have some amount of index coupling.
5. The phase condition has been derived for a symmetric cavity. In practice, lasers with cleaved facets are seldom symmetric, and there is a good chance that one of the two degenerate modes will have a more favorable phase condition. Although one of the modes will dominate and lase, it is not possible *a priori* to determine the lasing wavelength, and this particular mode may not have a high discrimination under all operating conditions. The second mode is usually not completely suppressed, and may dominate under a slightly different operating condition, for instance, a different bias current or temperature. Cleaved facets thus lead to poor single-mode yields in DFB lasers. Commercially, the front facet of a DFB laser is usually anti-reflection coated and the rear facet is high reflection coated. This breaks the mode degeneracy leading to a better single-mode performance. This also results in a higher front facet output power (compared to the cleaved facet case, where both the front and back facets both have equal reflectivities), which is essential for practical applications.

Similar to the phase condition, the absolute value of Eq. (23) is used to obtain the threshold condition for the DFB laser.

$$4(\alpha_0^2 + \delta^2) = \kappa\kappa^* e^{2\alpha_0 L} \qquad (26)$$

From Eq. (26) it can be seen that for a fixed value of κ, as the frequency deviation δ from the Bragg frequency increases, the threshold gain α_o also increases. This indicates that a larger gain is required for the higher-order modes to lase and, hence, the mode selectivity of the DFB lasers.

DEVICE CHARACTERISTICS

Light/Current Characteristics

Figure 3 shows the static light/current (*L*/*I*) and voltage/current (*V*/*I*) characteristics of a packaged DFB laser. The general form of the curves is similar to other semiconductor lasers. This particular DFB laser is meant for high-power fiber coupled applications and has a threshold current of 60 mA and an operating voltage of about 1.5 V. The *V*/*I* characteristics is similar to an electronic diode, and shows an exponential dependence of the injected current on applied voltage. The DFB laser in Fig. 3 is capable of operating at fiber coupled output powers as high as 50 mW.

DFB laser packaging styles vary from one manufacturer to another and the details are often trade secrets. Although the details may be different, there are three essential goals in any DFB package. The first is temperature stability. Single-mode characteristics of DFB lasers are very sensitive to temperature variations. The parameter of major concern is the variations in the emission wavelength with temperature. Most high-end DFB lasers are packaged with a thermoelectric cooler (TEC) for stabilizing the temperature.

The second goal is high coupling efficiency. Output power from the laser diode is expensive and careful attention is paid to maximize the amount of light that is coupled into a single-mode optical fiber pigtail. In manufacturing, fiber coupling efficiencies in the range of 60% can be obtained. This is achieved by a combination of laser diode design (to obtain a more uniform output spatial emission) and coupling lens design. Typically, a combination of a ball lens next to the laser facet (to correct any residual asymmetry in the emission profiles in the lateral and transverse directions to the facet) and a graded index (GRIN) lens at the entry point to the output fiber is used to couple light from the diode into the optical fiber.

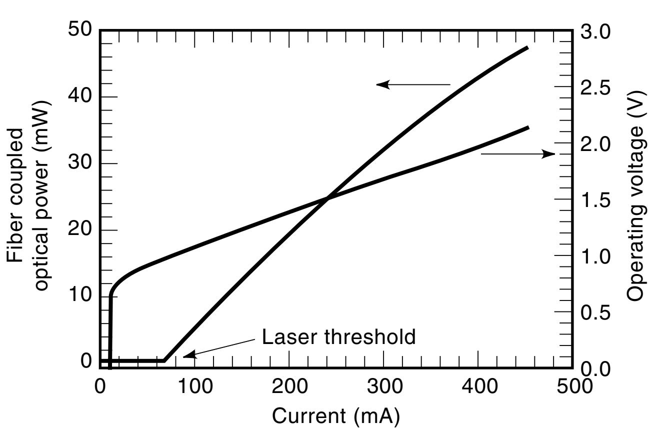

Figure 3. The *L*/*I* and *V*/*I* characteristics of the diode laser. At high drive currents, the series resistance of the diode dominates and the *V*/*I* curve tends to become more "linear." The output power does not continually increase with injected current. The *L*/*I* curve tends to "roll over" at high bias levels. This is due to thermal effects and is a common phenomenon in diode lasers.

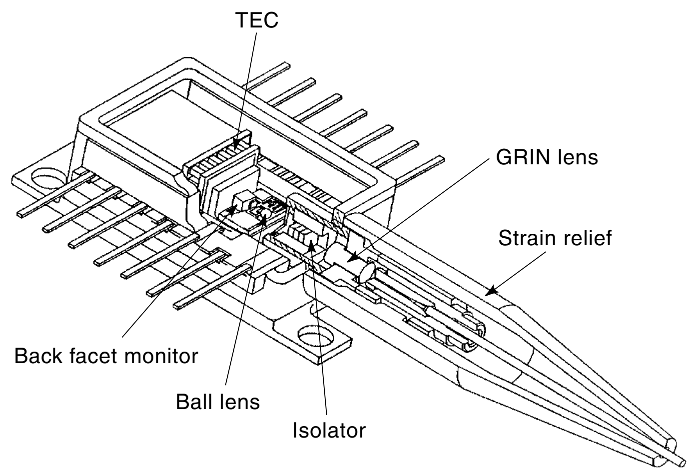

Figure 4. Cut-away drawing of a DFB laser in a "butterfly" style package. The laser diode itself is a small "speck" to the rear of the ball lens. The ball lens makes the spatial emission pattern of the DFB laser more symmetric. This is followed by the isolator and GRIN lens before the fiber. Strain relief prevents the misalignment of the fiber-coupling mechanism when the package pigtail is stressed during handling.

The third goal is to minimize the reflection of light back into the laser. As seen in the previous section, the wavelength stability of the DFB laser is governed by the wavelength-selective feedback provided by the grating structure. Any other spurious reflections, from the laser facet or from an external component in the fiber optic link, will lead to poor single-mode performance. Back reflection is minimized by properly anti-reflection-coating the lens surfaces and including an isolator in the package. Isolator is an optical device that allows light to be transmitted in one direction with very low loss, and essentially prevents light transmission in the reverse direction. The isolator may be placed after the ball lens and before the GRIN lens.

Figure 4 shows a drawing of a packaged DFB laser. This is the AT&T (now Lucent Technologies) Type 246 isolated laser module. The TEC is to the rear of the package, and the laser is mounted on an "L" bracket which is cooled by this TEC. There is a ball lens followed by an isolator and then a GRIN lens before the fiber pigtail, to couple the light output from the laser. The package also incorporates a laser back facet monitor, a *pin* photodiode, which measures the output power form the back facet of the laser. The photocurrent output from this detector can be appropriately scaled (if the relative facet coating levels are known) to accurately obtain the front facet or fiber coupled power. The feedback from back facet monitor is used to operate the DFB is a constant output power mode.

Optical Spectrum and Side Mode Suppression Ratio

Figure 5 shows the output spectrum of a DFB laser (for the same device whose static *L*/*I* and *V*/*I* characteristics are given in Fig. 3) at various current levels from below threshold. The output spectrum essentially builds up from noise below threshold to a single-mode output with an acceptable side mode suppression at about 20 mA to 30 mA above threshold. The multimoded output spectrum of a FP laser is shown for comparison. A number of competing optical modes are supported by the optical gain medium in a FP laser, and any one of the modes may dominate depending on the operating conditions, that is, the bias current and temperature.

Side mode suppression is a measure of the spectral purity of a DFB laser. Side mode suppression ratio (SMSR) or simply the mode suppression ratio (MSR) is the ratio of the power in the main oscillation peak to the power level in the most intense side mode (or the second most dominant mode). SMSR requirements are application specific, but a value in excess of 30 dB (> 1000) is considered desirable in a single-mode laser.

As shown in Fig. 5, SMSR of a DFB laser improves as the power in the main mode increases. Figure 6 shows the SMSR as a function of main mode power. It can be seen that SMSR in excess of 35 dB have been achieved at a fiber coupled power of 1 mW. This shows that DFB lasers are highly wavelength selective, and it takes very little power above threshold to achieve essentially single mode operation. Figure 6 also shows that SMSR increases linearly with main mode power

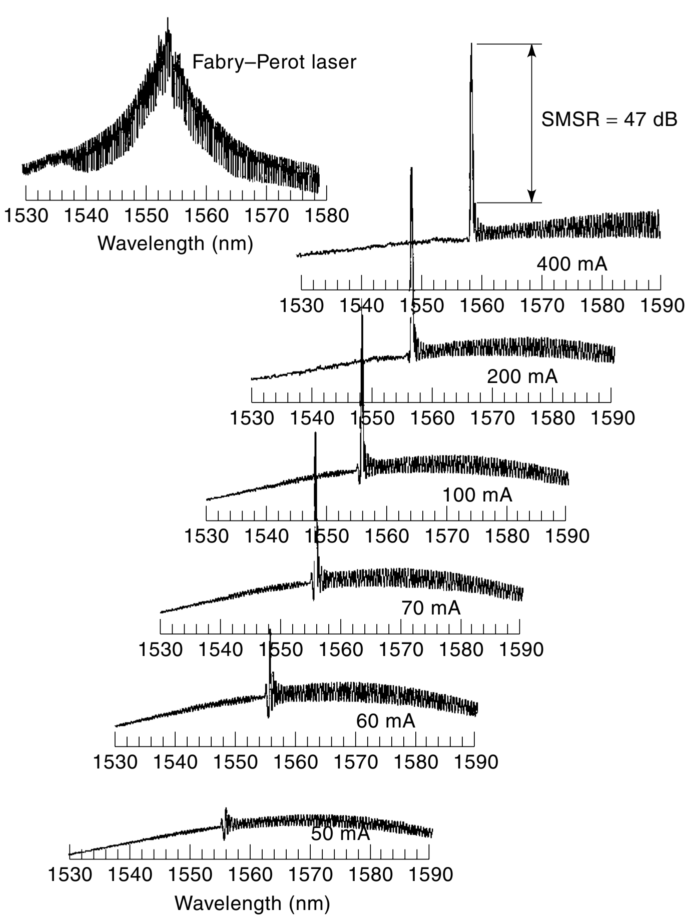

Figure 5. Spectral evolution of the DFB laser output at different bias current levels. The output builds from noise, and the single-mode characteristics are only well established at current levels above the threshold. The multimoded FP spectrum is provided for comparison.

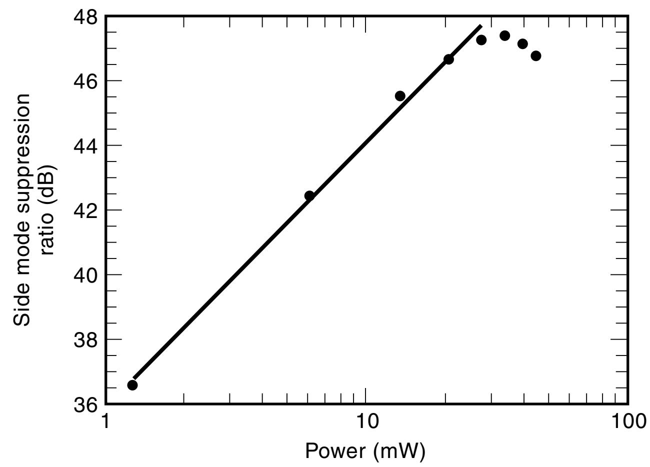

Figure 6. Dependence of the side mode suppression ratio (SMSR) on optical power. It takes very little output power to obtain a good SMSR. At high power levels, the SMSR begins to degrade due to nonlinear effects caused by high photon densities in the laser cavity.

(Fig. 6 is plot of log of SMSR vs. log of main mode power) up to a point before leveling off and eventually degrading at very high power levels. SMSR values up to 50 dB are possible in modern DFB lasers. The eventual degradation of the single-mode properties at very high power levels is a common characteristic of most DFB lasers. The grating structure in the DFB laser causes the optical field within the laser cavity to be nonuniform. This spatial nonuniformity leads to what is known as spatial hole burning (SHB) in the laser. These are localized areas in which the optical density is much higher than the average field in the cavity. The nonlinear effects due to SHB are complicated to analyze and are outside the scope of the treatment here.

The output spectrum in Fig. 5 shows a main oscillating peak on a background with some fine structure. There are two interesting features here. One is the fine structure itself and the other is that the main peak has been "pulled" to the left-hand side (shorter wavelength side) of the background, which gradually peaks at a much longer wavelength. The fine structure is the natural Fabry–Perot modes of the laser cavity, which have been suppressed by the presence of the grating. Second, the gradually increasing background is the natural gain spectrum of the active region. By adjusting the pitch of the grating structure, one can selectively control the oscillation wavelength of the DFB laser. This is called *detuning.* There are physical limits as to how much detuning may be used in a DFB laser. Forcing the DFB to operate at the extreme wavelength ends of the material gain may lead to unacceptable increases in the threshold current. Without going into the details, among other things, DFB lasers detuned to the shorter wavelength side generally have better high-speed modulation properties (5).

Great care is taken to suppress the natural Fabry–Perot modes of the cavity in a DFB laser. Figure 7 shows the *L*/*I* curve and the output spectrum of an "as cleaved" DFB laser. Laser facets or mirrors essential for laser action are formed by "breaking" the device along its crystal planes. These are natural cleavage planes and this process, referred to as cleaving, forms reflectors of outstanding optical quality. The facets of the DFB lasers are then coated to break the mode degener-

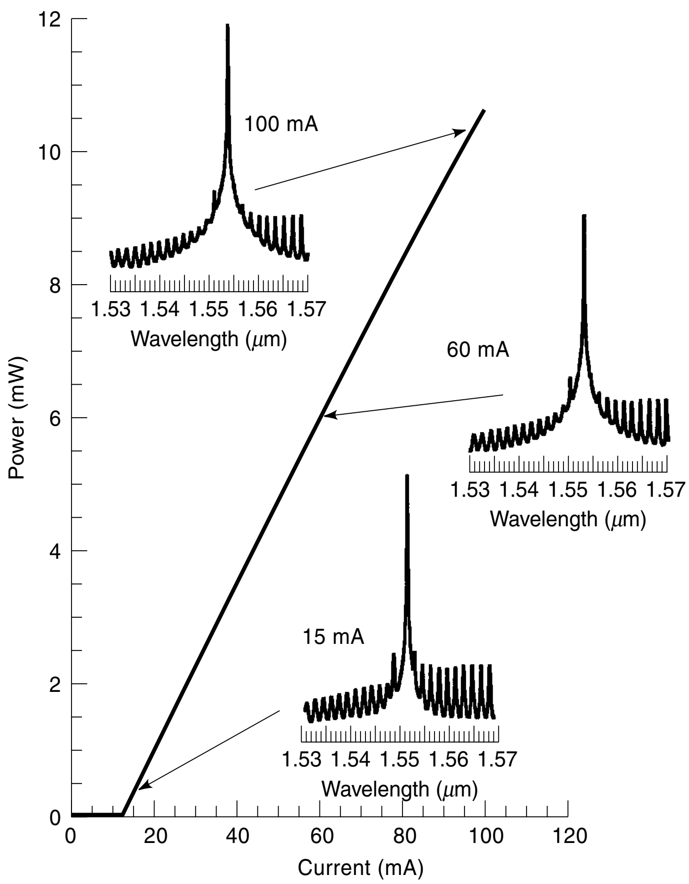

Figure 7. Output spectrum of an "as-cleaved" DFB laser. Although this laser is operating in a single longitudinal mode, its SMSR is poor compared to the case in Fig. 5. Since it is not possible to predict *a priori* which of the two degenerate modes will dominate, the single-mode yield, to a fixed wavelength specification, will be poor during manufacturing. This also shows that the single-mode operation of the DFB laser will degrade with feedback from an external surface (in this case it is the uncoated laser facet that is providing the unwanted feedback).

acy (see previous section). If the DFB lasers are operated uncoated, that is, as cleaved (Fig. 7), in addition to the competition between the two degenerate modes, one can also see the remnants of the natural FP modes of the cavity (the more pronounced spectral structure in the background compared to Fig. 5). SMSR for this structure is poor and will be strongly dependent on the operating conditions. Figure 7 also illustrates another problem with DFB lasers—their susceptibility to back reflections from an external source. As discussed earlier, care must be taken to eliminate back reflections in packaging these lasers.

Wavelength Stability and Tuning

In operation, both the temperature and bias current affect the output wavelength of a DFB laser. Figure 8 shows the effect of temperature on the operation wavelength of a DFB laser. This effect is also referred to as the temperature tuning of a DFB laser. One of the curves shows the wavelength variation with temperature at constant power and the other at constant bias current. Maintaining constant power at a higher temperature requires a higher bias current. There are two effects that lead to this wavelength increase. The dominant one is the variation of the mode index (material properties) with temperature. There is also a small carrier-induced contribution to the mode index. As the temperature increases, the larger bias current required for DFB operation at constant power, causes a corresponding increase in the carrier density within the laser cavity (6). These two effects are differentiated in the two curves presented in Fig. 8.

The wavelength tuning (slope of the plot) with temperature of the DFB laser in Fig. 8, at constant bias, is about 0.09 nm/°C. For constant power operation, it is about 0.10 nm/°C. The slope is higher for the constant power operation, since it also includes the effect of the increased carrier density on the mode index. As is obvious by now, DFB lasers can also be current tuned. Figure 9 shows the variation is operating wavelength with bias current at room temperature. Although the relationship is not linear, the wavelength increases (approximately) at a rate of 0.1 nm for every 10 mA increase in bias current. Tuning range of the order of 1 nm to 2 nm is possible with either technique. A combination of current and temperature tuning is used in practice to operate DFB lasers at precisely defined wavelengths.

Linewidth

Another measure of spectral purity of a DFB laser is the laser linewidth. This is usually defined as the full width at half maximum (FWHM) power of the main oscillating mode. It is expressed in frequency units of kHz. Under steady-state constant bias (also called the continuous wave or CW) operation, the linewidth is a measure of the laser phase noise (frequency noise). There is additional broadening of this intrinsic linewidth under modulation due to other cavity mechanisms. Linewidth of a few hundred kHz (<1 MHz) is desirable in good DFB lasers.

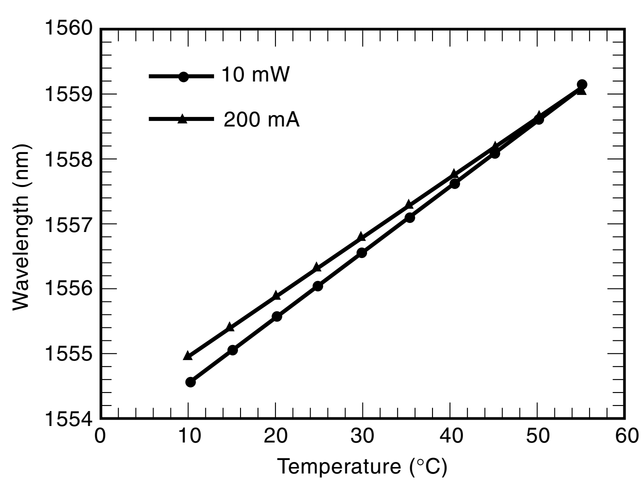

Figure 8. Temperature tuning curves at constant current and constant output power. Additional bias current is required to maintain constant output power from the DFB laser at high temperatures. At these higher bias levels, the additional index variation caused by the increased carrier density causes the constant power tuning curve to have a higher slope.

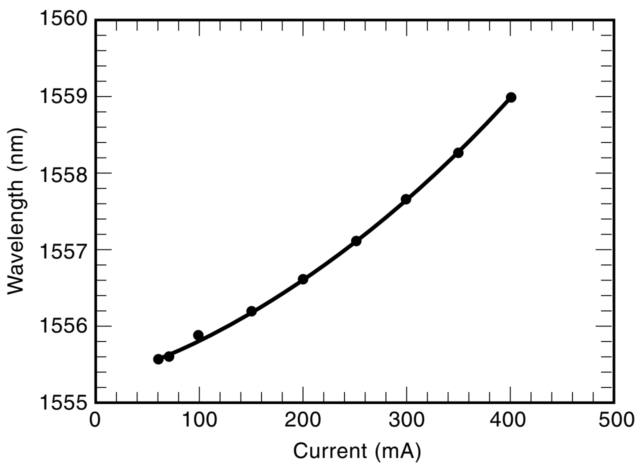

Figure 9. Wavelength tuning of the DFB laser with bias current at constant temperature.

Theory of noise in semiconductor lasers is complicated (7). The major contribution to noise in all laser systems is spontaneous emission. This is the result of adding the spontaneous emission field which has random phase to the coherent oscillating field of the laser cavity. The second contribution, which is peculiar to semiconductor lasers, is the index variations in the laser cavity caused by carrier density fluctuations. Without going into the details of the mathematical formulation worked out by Henry (8), the proportionality relationship for the linewidth of a semiconductor may be written as in Eq. (27).

$$\Delta f \propto \frac{(1+\alpha^2)}{P_0} \tag{27}$$

Equation (27) shows that the laser linewidth is inversely proportional to the output power P_0. The $(1 + \alpha^2)$ factor is referred to as the enhancement to the *modified* Schawlow–Townes expression for the laser linewidth. This enhancement is the result of carrier density fluctuation, and α, which is called the linewidth enhancement factor is defined as in Eq. (28):

$$\alpha = -\frac{4\pi}{\lambda}\left(\frac{dn/dN}{dg/dN}\right) \tag{28}$$

The linewidth enhancement factor is proportional to the ratio of the index variation with carrier density to the gain variation with carrier density (also called the differential gain). α (which should be confused with the notation used for the material gain in the previous section) is a material parameter and is influenced by the design (dimensions and doping levels) of the active region. It is desirable to keep this parameter as small as possible. Typical values for α in DFB lasers are less than 5 with good DFB lasers having α values less than half that number. Linewidth as a function of inverse optical power for a commercial DFB module is shown in Fig. 10. The same plot gives the best linewidth data of 3.6 kHz reported to date for a solitary DFB laser (9). The point is made about the solitary diode because the linewidth of the semiconductor laser can be further reduced by using external feedback techniques for noise reduction.

Direct current modulation of the DFB laser will broaden its linewidth. The current modulation of the active region modulates both the photon and carrier density in the cavity. Modulation of the carrier density modulates the mode index, which results in varying the effective cavity length. This leads to a variation in the resonant oscillation frequency or the broadening of the laser linewidth. This process is called laser "chirp." An expression can be written for the transient (time dependent) chirp that occurs during current modulation of the laser as in Eq. (29) (10).

$$\Delta v(t) = \frac{\alpha}{4\pi}\left(\frac{1}{P_0(t)}\right)\left(\frac{dP_0(t)}{dt}\right) \tag{29}$$

Chirp in a laser is proportional to the linewidth enhancement factor and the rate of change of optical power (equivalently the modulation or data rate). Laser chirp under current modulation is a general property of all semiconductor lasers and is not peculiar to DFB lasers alone. Since laser chirp combined with fiber dispersion, will limit the practical transmission distance in fiber optic systems, great care is taken to design DFB lasers with minimum amount of chirp under modulation, that is, with small α parameters. Since laser chirp is "unavoidable," single-frequency DFB lasers are not directly modulated in long-distance transmission systems. Instead, an external modulator, which can be independently optimized for low chirp, is used to modulate data onto the optical carrier.

Intensity Noise

In addition to phase noise, there is also intensity noise in a diode laser. At constant bias, the laser output power fluctu-

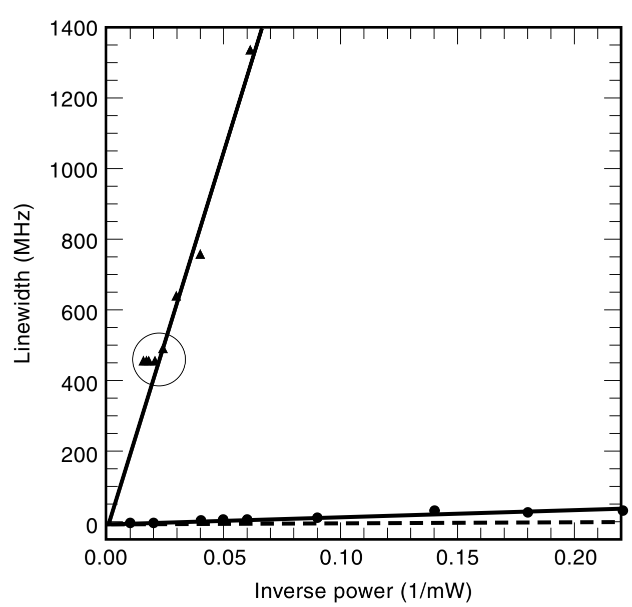

Figure 10. Linewidth measured on a commercial DFB laser package (solid triangles) compared to what has been reported for some of the best DFB laser diodes in the world (solid circles).

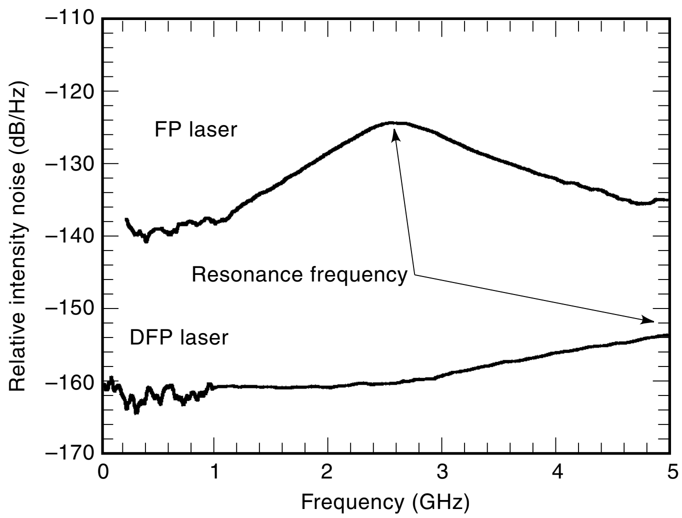

Figure 11. Comparison of the relative intensity noise (RIN) for a FP and DFB laser. The "humps" in the curve are due to the resonant enhancement of noise, which is a consequence of the nonlinear interaction of electrons and photons in the laser cavity.

ates with time about its steady-state value. The random carrier recombination and photon generation events produce instantaneous time variations in the carrier and photon densities, even in the absence of current modulation or other external disturbances. This fluctuation in the laser output intensity is called the relative intensity noise (RIN) and is written as in Eq. (30):

$$\mathrm{RIN} \equiv \frac{\langle \Delta P(t)^2 \rangle}{\langle P_0 \rangle^2} \tag{30}$$

where $\langle P_0 \rangle$ is the time averaged output power and $\Delta P(t)$ is the instantaneous variation in the average output power. RIN is normalized to per unit bandwidth and is commonly expressed in log units as decibels per hertz. DFB lasers have a much lower level of RIN than FP lasers. The major source of RIN enhancement in FP lasers is the mode competition between multiple longitudinal modes of the cavity, which leads to intensity fluctuations. This is known as the mode partition noise. Unlike the DFB lasers, the carriers that recombine in a FP laser can generate a photon in any one of the modes supported by the laser cavity. Figure 11 shows the RIN for a DFB and a FP laser. A good DFB laser designed for analog applications, like the cable television transmission systems, must have RIN at or below −160 dB/Hz. FP lasers generally have 20 dB to 30 dB higher RIN, but these levels are tolerable for most digital applications.

The RIN spectrum for both the DFB and FP lasers have a distinct hump, called the resonance peak, which occurs at what is known as the resonance frequency. The resonance phenomenon is a result of the nonlinear carrier–photon interaction in the laser cavity. The resonance frequency is larger in cavities with larger photon densities. It is also larger in active regions with a larger differential gain. For low levels of intensity noise, the laser should have as large a resonance frequency as possible and be operated at high output power levels. It is also good to have a large resonance frequency for high-speed lasers, because the intrinsic modulation bandwidth of the laser is proportional to the resonance frequency.

BIBLIOGRAPHY

1. I. P. Kaminow and T. L. Koch (eds.), *Optical Fiber Telecommunications IIIA–IIIB,* New York: Academic Press, 1997.
2. L. A. Coldren and S. W. Corzine, *Diode Lasers and Photonic Integrated Circuits,* New York: Wiley, 1995.
3. G. P. Agrawal and N. K. Dutta, *Semiconductor Lasers,* 2nd ed., New York: Van Nostrand Reinhold, 1993.
4. H. Kogelnik and C. V. Shank, Coupled-wave theory of distributed feedback lasers, *J. Appl. Phys.,* **43** (5): 2327–2335, 1972.
5. R. Nagarajan, D. Tauber, and J. E. Bowers, High Speed Semiconductor Lasers, in T. P. Lee (ed.), *Current Topics in Electronics and Systems, Vol. 1—Current Trends in Integrated Optoelectronics,* Singapore: World Scientific, 1994, pp. 1–44.
6. S. Akiba et al., Temperature dependence of lasing characteristics of InGaAs/InP distributed feedback lasers in 1.5 μm range, *Japan. J. Appl. Phys.,* **21** (12): 1736–1740, 1982.
7. K. Petermann, *Laser Diode Modulation and Noise,* Dordrecht: Kluwer, 1988.
8. C. H. Henry, Theory of linewidth of semiconductor laesrs, *IEEE J. Quantum Electron.,* **QE-18** (2): 259–264, 1982.
9. M. Okai et al., Corrugation-pitch-modulated distributed feedback lasers with ultra-narrow spectral linewidth, *Japan. J. Appl. Phys., Part 1,* **33** (5A): 2563–2570, 1994.
10. T. L. Koch and J. E. Bowers, Nature of wavelength chirping in directly modulated semiconductor lasers, *IEE Electron. Lett.,* **20** (25/26): 1038–1040, 1984.

RADHAKRISHNAN NAGARAJAN
SDL, Inc.